

Pixel Design Utilized P-type Substrate to Achieve Superior NIR Sensitivity and Resolution with Low Dark Noise

Takanori Usuki, Masayuki Saeki, Takefumi Konishi, Hiroshi Iwata, Kenichi Nagai, and Toshio Yoshida
Semiconductor Business Unit, Sharp Fukuyama Semiconductor Co., Ltd.,
Fukuyama-shi, Hiroshima 721-0921, Japan
E-mail: usuki.takanori@sharp.co.jp **Phone:** +81-50-5433-5181

1. INTRODUCTION

Recently, the demand for CMOS Image Sensor (CIS) has been transitioning from pixel shrink to install additional functions such as global shutter and 3D-imaging technology. In particular, 3D-imaging technology has a great potential to change the appearance of CIS markets and it has been developed all over the world. 3D-CIS are often adopted with 850 nm or 940 nm irradiation because it is less affected by background light. Therefore, high Near Infra-Red (NIR) sensitivity are strongly required. However, Quantum Efficiency (QE) of the conventional pixel structure using n-type epitaxial layer (epi-layer) is about 20 % (@ 850 nm). As the one way for achieving high NIR sensitivity, a thicker p-type epi-layer is adopted, but there is a problem that resolution deteriorates [1]. Generally, in order to achieve high NIR sensitivity and resolution, it is thought that depletion region must be expanded with the impurity concentration of epi-layer under $1 \times 10^{14} \text{ cm}^{-3}$ [2].

According to the results of this study, despite setting the impurity concentration of epi-layer under $1 \times 10^{14} \text{ cm}^{-3}$ and extending the depletion region have almost no effect on improvement of NIR sensitivity, the characteristics in dark condition and the resolution are significantly deteriorated. In this study, by increasing the impurity concentration of epi-layer, we have demonstrated superior NIR sensitivity and resolution while suppressing deterioration of the characteristics in dark condition using the results of measurement and the theoretical calculation.

2. CALCULATION METHOD

2.1 Calculation method of QE

In the calculation QE of this study, the reflectance of multi-layer on the Si substrate, the light absorption of Si epi-layer and the diffusion current due to carriers generated in the Si epi-layer are considered (Figure 1).

We assumed that, all electrons generated in the photodiode n-type region and the depletion region contribute to photocurrent, and a part of electrons generated in the diffusion region is lost by recombination and the other electrons reaching the depletion region by diffusion contribute to photocurrent. Then the total photocurrent density is expressed by following formula.

$$J_{ph} = -\frac{qI_0\lambda}{hc} \left[1 - \frac{\exp(-\alpha Z_{dep})}{1 - \alpha^2 L_n^2} \cdot \left(1 - \alpha L_n \frac{\cosh\left(\frac{Z_{dif}}{L_n}\right) - \exp(-\alpha Z_{dif})}{\sinh\left(\frac{Z_{dif}}{L_n}\right)} \right) \right] \quad (1)$$

Here, the reflectance of multi-layer structure as shown in Figure 1 is able to calculate using characteristics matrix of each layer expressed M . Therefore, when incident light is s-polarization, R of the reflectance is estimated with following formula by obtaining relationship between electric field and magnetic field at the incident medium/first layer($z=0$) interface and the m-th layer/ Si substrate($z=L_s$) interface.

$$R = |r|^2, \quad r = \frac{\eta_0 M_{11} - \eta_0 \eta_s M_{12} + M_{21} - \eta_s M_{22}}{\eta_0 M_{11} - \eta_0 \eta_s M_{12} - M_{21} + \eta_s M_{22}} \quad (2)$$

However, after passing through the multi-layer, light propagates to the substrate having refractive index n_s as shown in Figure 1. In case of p-polarized incident light, the reflectance can be similarly obtained [3].

Using the total photocurrent density J_{ph} and the reflectance R of multi-layer in above, QE can be calculated by the following formula.

$$QE = \left| \frac{J_{ph}(1-R)}{qI_0\lambda/hc} \right| \times 100 \quad (3)$$

However, we assumed that electrons generated in the region shallower than potential peak of the surface pinning region are recombined at the surface.

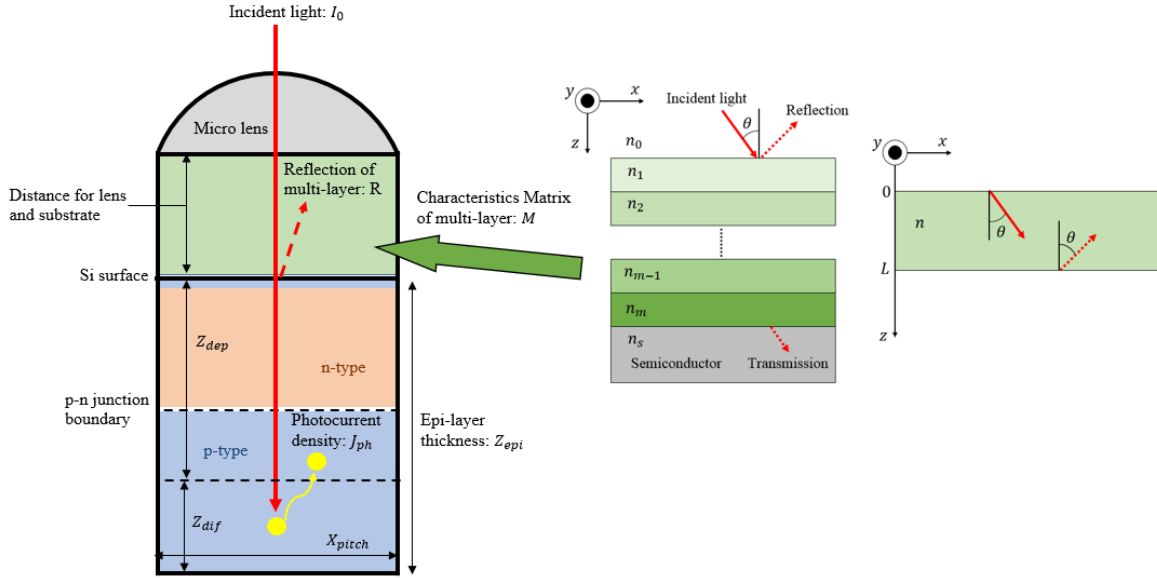


Figure 1. Schematic of unit pixel for calculation QE and the physical phenomenon of inside.

2.2 Estimation of dark current

Generally, when it is not necessary to apply a large applied voltage like the avalanche photodiode, the dark current is composed of three current components: diffusion current, generated current, and leakage current without tunneling current.

$$\begin{aligned}
 I_{dark} &= I_{dif} + I_{gen} + I_{leak} \\
 &= \frac{qD_n A}{L_n P_p} N_c N_v \exp\left(-\frac{E_g}{kT}\right) + \frac{q w A}{2\tau_g} \sqrt{N_c N_v} \exp\left(-\frac{E_g}{2kT}\right) + \frac{q\sigma v_{th} N_{st} A_s}{2} \sqrt{N_c N_v} \exp\left(-\frac{E_g}{2kT}\right) \quad (4)
 \end{aligned}$$

A : p-n junction area, D_n and L_n : the diffusion coefficient and the diffusion length of electrons, P_p : hole concentration in p-region, N_c and N_v : density of state in conduction band and valence band, E_g : band gap, w : width of depletion layer, τ_g : effective lifetime of carriers in depletion layer, N_{st} and σ : the density of defect and the capture cross-section in depletion layer respectively, v_{th} : thermal velocity of carriers, A_s : p-n junction area at interface.

3. MEASUREMENT AND CALCULATION

3.1 Optimization with p-type epi-layer conditions

Figure 2 shows that QE spectra comparison between measurement results and theoretical calculation with different epi-layer conditions. According to this result, we can be understood that the results of measurement and theoretical calculation for n-type and p-type substrates are matched in all wavelength regime. And, we can be seen that NIR sensitivity increases with thicker epi-layer, and it hardly depends on the impurity concentration. Furthermore, QE has been achieved 46 % (@ 850 nm) with the 15 μm epi-layer. On the other hand, Figure 3 shows the measurement results of resolution under NIR irradiation with different thickness and impurity concentration. From these results, the resolution deteriorates sharply by decreasing the impurity concentration rather than increasing the thickness of epi-layer. Consequently, by increasing the impurity concentration of epi-layer, we confirmed that the resolution was not greatly deteriorated even in NIR regime.

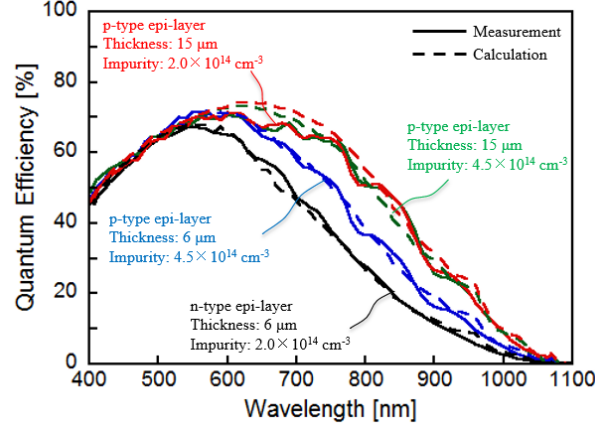


Figure 2. QE spectra comparison between measurement results and theoretical calculation with different epi-layer conditions.

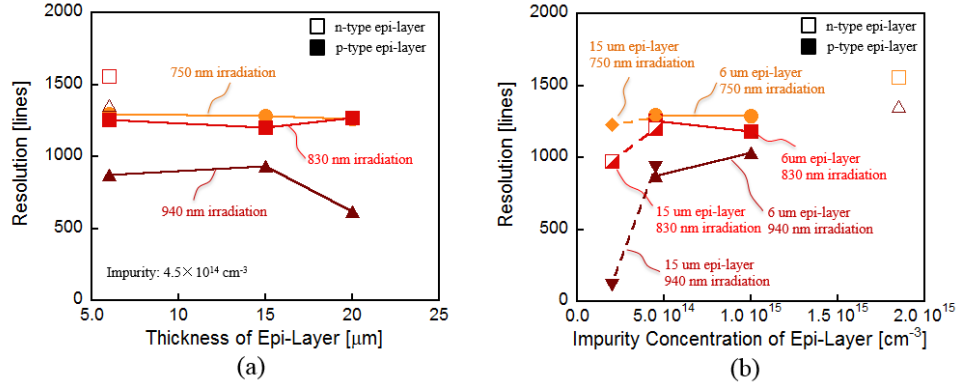


Figure 3. Results of measurement resolution under NIR irradiation with different (a) thickness and (b) impurity concentration of epi-layer.

3.2 Investigation of characteristics with dark condition

Figure 4(a) shows the dark current temperature dependence between measurement results and theoretical calculation with n-type and p-type substrate. This result shows the usefulness of theoretical calculation because measurement result and theoretical calculation match well for both of n-type and p-type substrate. We can be seen that the dark current at high temperature is degraded by the adoption of the p-type substrate as compared with the n-type substrate. This is because the reduction of the hole concentration in deep p-type region and the addition of the diffusion current component that is hardly present with the n-type substrate.

Here, for the discussion, Figure 4(b) shows the result of dark current components analysis in theoretical calculation. From this, we can be understood that the dark current at room temperature is mainly composed of diffusion current.

Figure 5 shows the impurity concentration dependence of the dark current and the dark noise with measurement results and theoretical calculation. According to these results, the characteristics in dark condition are significantly deteriorating at lower impurity concentration. Considering from the physical model applied to the theoretical calculation, this is because the diffusion current and the generated current increased due to decreasing the hole concentration in the diffusion region and expanding the depletion region.

When the dark current of equation (4) is differentiated by P_p and w , the following equation is obtained.

$$\Delta I_{dark} = -\frac{qD_n A}{L_n P_p^2} N_c N_v \exp\left(-\frac{E_g}{kT}\right) \cdot \Delta P_p + \frac{qA}{2\tau_g} \sqrt{N_c N_v} \exp\left(-\frac{E_g}{2kT}\right) \cdot \Delta w \quad (5)$$

According to equation (5), the term of diffusion current component is proportional to square of hole concentration of p-type region, and does not substantially affect dark noise if the hole concentration in the p-type region is high

enough. On the other hand, although the term of generated current component deteriorate dark noise due to the expansion of depletion region, it is thought that contribution to noise deterioration due to the increase of generated current is small because diffusion current is main component at room temperature. Therefore, if the hole concentration in p-type region is about $1 \times 10^{15} \text{ cm}^{-3}$, it hardly affects deterioration in the image quality due to the adoption of a thick p-type substrate.

Furthermore, the characteristics in dark condition with 15 μm epi-layer are better than 6 μm epi-layer. As considering Figure 4(C) showing a schematic of dark current generation model with p-type substrate, this is because many defects in the p⁺⁺-type substrate (under the epi-layer) are far away from n-type region of photodiode. On the other hand, the characteristics in dark condition with 20 μm epi-layer are more deteriorated than 15 μm epi-layer due to expanding the diffusion region.

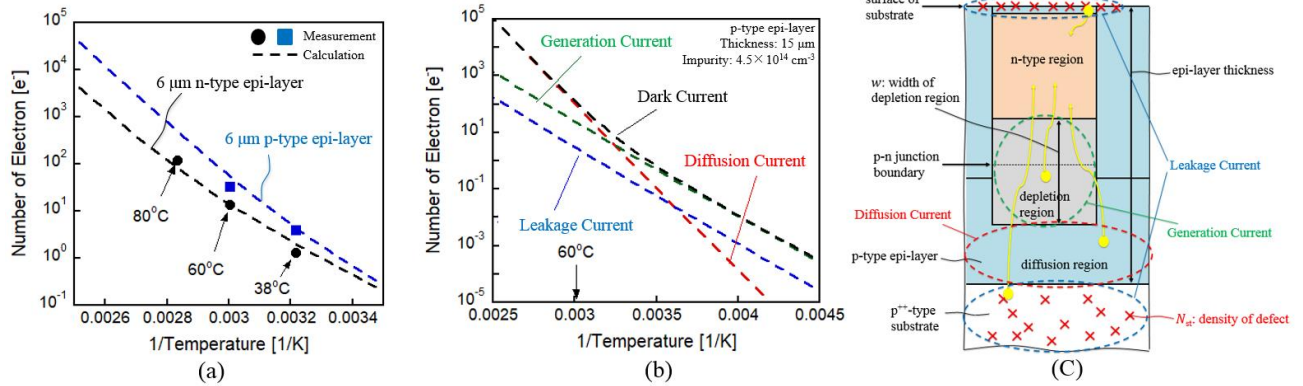


Figure 4. (a)Results of the dark current with measurement and theoretical calculation. (b)Analysis of dark current components for theoretical calculation. (C) Schematic of dark current generation model with p-type substrate

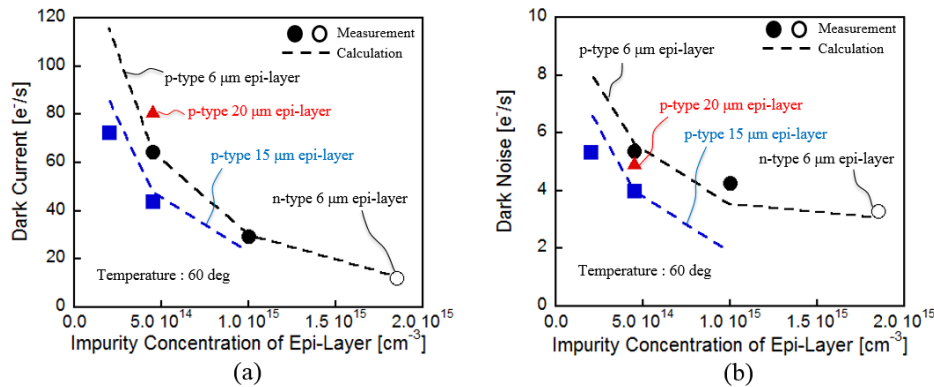


Figure 5. Impurity concentration dependence of (a)the dark current and (b)the dark noise with measurement and theoretical calculation.

4. CONCLUSION

We had been able to construct our novel models to calculate because we had not be concerned with a general concept. As a result, if we use our novel models, we can get superior performance for NIR sensitivity, resolution, and characteristics in dark condition without any prototype.

REFERENCES

- [1] Lahav, A., Veinger, D., Birman, A., Suzuki, M., Hirata, T., Tachikawa, K., Tsutsui, M., Yokoyama, T, Nishi, Y. and Mizuno, I., "Cross Talk, Quantum Efficiency, and Parasitic Light Sensitivity comparison for different Near Infra-Red enhanced sub 3 μm Global Shutter pixel architectures," IISW2017 R56
- [2] <http://www.ekouhou.net/%E5%A2%97%E5%B9%85%E5%9E%8B%E5%9B%BA%E4%BD%93%E6%92%AE%E5%83%8F%E8%A3%85%E7%BD%AE/disp-A.2010-56345.html>
- [3] <http://www.yoshioka-lab.com/document/opticalresponse/multilayer/transfermat.pdf>